Reflectionless Multichannel Wavelength Demultiplexer in a Transmission Resonator Configuration

Chongjun Jin, Shanhui Fan, Shouzhen Han, and Daozhong Zhang

***Abstract*—A wave demultiplexer system with N channels in a two-dimensional photonic crystal is proposed. The demultiplexer is realized by the coupling among an ultra-low-quality factor microcavity and N resonators with high-quality factor. The coupling mode theory is employed to analyze the behavior of this system. The analytic results reveal that the reflection is fully absent at the peak frequencies for all channels. The simulations obtained by multiple-scattering method and experimental results in the microwave region show that the analysis is valid. This method might also be valuable for the design of other all-optical functional circuits.**

***Index Terms*—Microcavity, photonic crystal, resonant couple, wavelength-demultiplexer.**

I. Introduction

WAVELENGTH demultiplexers play an important role in enhancing the capacity of optical communications. Commercially available wavelength demultiplexer systems, such as planar lightwave circuit-based array waveguide gratings [1]–[3] and fiber gratings [4], tend to occupy a footprint of at least one centimeter square. There is therefore tremendous interest in developing devices that are more compact.

Recently, photonic crystal based wavelength demultiplexers attracted much attention [5]–[11] as potentially viable schemes for device miniaturization. Photonic crystals are artificial structures composed of periodically arrayed dielectric media [12], [13]. These structures have been found to be very useful in the design of all-optical devices [14]. For wavelength demultiplexer applications, photonic-crystal-based mechanisms that have been proposed include the channel-drop tunneling scheme [5]–[7], the super-prism effect [11], and the frequency-selective dropping of photons from waveguide channel to the surrounding media [8]–[10]. Among all of these mechanisms, the most compact configurations involve the interactions of waveguides with microcavities [5]–[10]. For practical implementations, however, it is crucial that the reflection be eliminated. Previously, the elimination of reflection is achieved by *side coupling* the cavity to the waveguides, and by adjusting the symmetry properties of the cavity modes [5]. Doing so, however, tends to require detailed tunings of the cavity properties, which represent a challenge in device designs and fabrications.

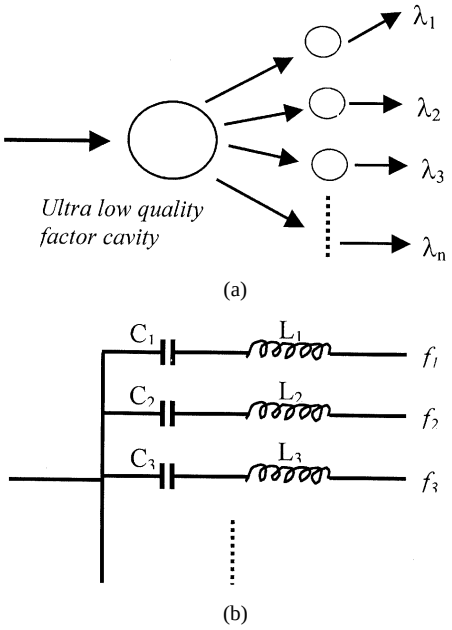

Fig. 1. (a) Schematic optical circuit for realizing a wave demultiplexer with multichannel. (b) Schematic electronic circuit of the multichannel filter.

In this paper, we introduce a photonic crystal demultiplexer structure based upon the coupling among a microcavity with an ultra-low-quality factor and *transmission resonators* with high-quality factors, as shown schematically in Fig. 1(a). The configuration consists of N transmission resonators, N branches, and a microcavity with low-quality factor. Each resonator possesses a resonant frequency at a particular signal frequency channel, to allow for a frequency-selective transmission of the frequency channel into the corresponding waveguide. In general, in transmission resonator configurations, signals at frequency channels away from the resonant frequency are reflected. Here, however, we introduce a theoretical criterion to show that by appropriate design of the waveguide branches, the overall reflection from the demultiplexer device can, in fact, be completely eliminated for all frequency channels. We substantiate our theoretical analysis with numerical and experimental work. In such, our design represents an optical analog of a classic electronic filter circuit, as shown in Fig. 1(b), where N channels can be perfectly separated by N inductance–capacitance (LC) resonant circuits with near 100% efficiency and no reflections [15].

Manuscript received January 31, 2002; revised August 13, 2002. This work was supported by the NNSFC, by the Chinese National Key Basic Research Special Fund (CNKBRSF), and by the National Research Center for Intelligent Computing Systems under Grant 99 104.

C. Jin, S. Han, and D. Zhang are with the Optical Physics Laboratory, Institute of Physics and Center for Condensed Physics, Chinese Academy of Sciences, Beijing, 100080, China.

S. Fan is with the Department of Electrical Engineering, Stanford University, Stanford, CA 94305-4085 USA.

Digital Object Identifier 10.1109/JQE.2002.806188

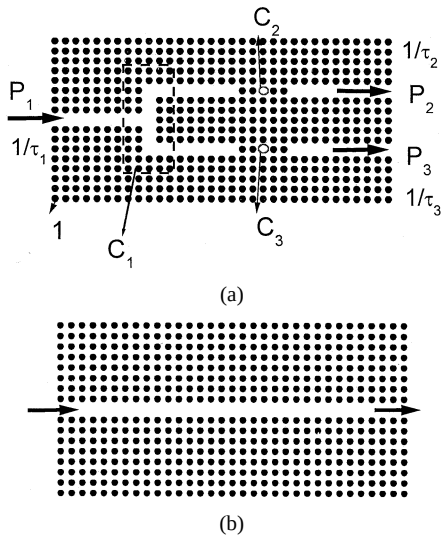

Fig. 2. (a) Cross section of the wave demultiplexer with two channels composed of two-dimensional photonic crystal. (b) Corresponding straight waveguide.

Let us start by considering the case with only two channels before we generalize the analysis to N channels. We consider a structure consisting of an input waveguide split into two outgoing waveguides at a T-branch, as shown in Fig. 2(a). Within each outgoing waveguide, we place a resonator, labeled C_2 and C_3, respectively. Each of the resonators is symmetrical with two cylinders at either side of the defect cylinder. Furthermore, the T-branch waveguide and the bent waveguides can be considered as an ultra-low-quality factor microcavity, labeled as C_1 [16]. Therefore, we can describe the whole optical system in terms of the coupling among the three microcavities, and deduce its properties using coupled mode theory. As the losses of the cavities can be designed to be very small, and the coupling between the cavities C_2 and C_3 is negligible, the coupling equations can be written as [17]

$$\frac{da_1}{dt} = j\omega_1 a_1 - a_1\frac{1}{\tau_1} + S_{+1}\sqrt{\frac{2}{\tau_1}} + \kappa_{12}a_2 + \kappa_{13}a_3 \quad (1)$$

$$\frac{da_2}{dt} = j\omega_2 a_2 - a_2\frac{1}{\tau_2} + \kappa_{21}a_1 \quad (2)$$

$$\frac{da_3}{dt} = j\omega_3 a_3 - a_3\frac{1}{\tau_3} + \kappa_{31}a_1 \quad (3)$$

$$S_{-1} = -S_{+1} + \sqrt{\frac{2}{\tau_1}}a_1,\ S_{-2} = \sqrt{\frac{2}{\tau_2}}a_2$$

$$S_{-3} = \sqrt{\frac{2}{\tau_3}}a_3 \quad (4)$$

where ω_i and a_i are the resonant frequencies and the amplitudes of the resonant modes for C_i ($i = 1, 2, 3$), respectively, $1/\tau_i$ is the decay rate of the microcavity C_i due to the power escape through the port P_i, S_{-i} and S_{+i} denote the field amplitudes of the input and output waves at the port P_i, respectively, and κ_{ij} represents the coupling coefficient between resonant cavities.

Using (1)–(4), the transmittivity t_2 and t_3 at the ports P_2 and P_3, respectively, and the reflectivity r, can be determined as in (5)–(7), shown at the bottom of the page.

For a full demultiplexing operation in a wavelength-division-multiplexing (WDM) system, we would like to completely transmit each frequency channel to an appropriate corresponding output waveguide without any reflection or crosstalk. In this two-channel WDM device, therefore, we will be primarily interested in the response function of the system in the vicinity of the resonant frequencies ω_2 and ω_3. Ideally, we would like the reflectivity to vanish, i.e., $r = 0$, for both frequency channels ω_2 and ω_3. Also, at each frequency channel ω_2 or ω_3, we would like the corresponding transmittivity, t_2 or t_3, respectively, to reach 100%, while the other transmittivity becomes zero, in order to eliminate crosstalk. From (5)–(7), shown at the bottom of the page, one could easily check that this ideal behavior can be achieved provided that the following three criteria are satisfied:

$$\omega_m - \omega_1 \ll 1/\tau_1 \quad (8)$$

$$|j(\omega_2 - \omega_3) + 1/\tau_3| \gg |j(\omega_2 - \omega_2) + 1/\tau_2| = 1/\tau_2 \quad (9)$$

$$\kappa_{1m} = \kappa_{m1} = j/\tau_1\tau_m. \quad (10)$$

Here, in (8) and (10), $m = 2, 3$ represents the label for the cavities in the outgoing waveguides.

Let us give a brief physical discussion of each of these three criteria above. Equation (8) indicates that the frequency channels of the signals should fall within the resonant line shape

$$t_2 = \left|\frac{S_{-2}}{S_{+1}}\right|^2 = \left|\frac{\frac{2\kappa_{21}}{\sqrt{\tau_1\tau_2}}}{\left[j(\omega-\omega_1)+\frac{1}{\tau_1}\right]\left[j(\omega-\omega_2)+\frac{1}{\tau_2}\right] + \kappa_{21}\kappa_{12} + \kappa_{31}\kappa_{13}\frac{\left[j(\omega-\omega_2)+\frac{1}{\tau_2}\right]}{\left[j(\omega-\omega_3)+\frac{1}{\tau_3}\right]}}\right|^2 \quad (5)$$

$$t_3 = \left|\frac{S_{-3}}{S_{+1}}\right|^2 = \left|\frac{\frac{2\kappa_{31}}{\sqrt{\tau_1\tau_3}}}{\left[j(\omega-\omega_1)+\frac{1}{\tau_1}\right]\left[j(\omega-\omega_3)+\frac{1}{\tau_3}\right] + \kappa_{31}\kappa_{13} + \kappa_{21}\kappa_{12}\frac{\left[j(\omega-\omega_3)+\frac{1}{\tau_3}\right]}{\left[j(\omega-\omega_2)+\frac{1}{\tau_2}\right]}}\right|^2 \quad (6)$$

$$r = \left|\frac{S_{-1}}{S_{+1}}\right|^2 = \left|\frac{-j(\omega-\omega_1)+\frac{1}{\tau_1}}{j(\omega-\omega_1)+\frac{1}{\tau_1}} + \frac{\left[\kappa_{12}t_2\sqrt{\frac{\tau_2}{\tau_1}} + \kappa_{13}t_3\sqrt{\frac{\tau_3}{\tau_1}}\right]}{j(\omega-\omega_1)+\frac{1}{\tau_1}}\right|^2 \quad (7)$$

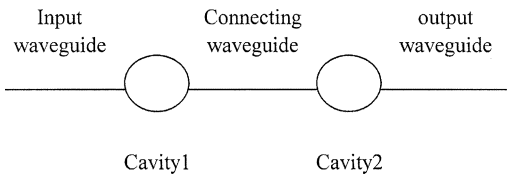

Fig. 3. Schematic picture of the coupling between two resonators.

of the branch; this should hold true for any broad-band splitter structures [14]. Equation (9) requires that the microcavities C_2 and C_3 should possess sufficiently high-quality factors in order to provide the necessary distinction between nearest neighbor channels. Such a requirement is typically satisfied for any WDM microcavity filter structure. The key designing consideration is then encapsulated in (10). Simply put, this equation relates the coupling constants between the cavities to the decaying rate of the cavities to each individual port.

We shall now see how (10) can be satisfied, by considering the coupling constant between two cavities that are connected with a waveguide, as shown in Fig. 3. Our treatment closely follows Haus and Lai's theory on coupled cavity structures [18]. Briefly, the coupled-mode theory equations that describe the structure in Fig. 3 are

$$\frac{da_1}{dt} = j\omega_1 a_1 - a_1\frac{1}{\tau_1} - a_1\frac{1}{\tau_1'} + S_{+1}\sqrt{\frac{2}{\tau_1}} + S'_{+1}\sqrt{\frac{2}{\tau_1'}} \quad (11)$$

$$\frac{da_2}{dt} = j\omega_2 a_2 - a_2\frac{1}{\tau_2} - a_2\frac{1}{\tau_2'} + S_{+2}\sqrt{\frac{2}{\tau_2}} + S'_{+2}\sqrt{\frac{2}{\tau_2'}} \quad (12)$$

$$S_{-1} = -S_{+1} + \sqrt{\frac{2}{\tau_1}}\,a_1 \quad (13)$$

$$S'_{-1} = -S'_{+1} + \sqrt{\frac{2}{\tau_1'}}\,a_1 \quad (14)$$

$$S_{-2} = -S_{+2} + \sqrt{\frac{2}{\tau_2}}\,a_2 \quad (15)$$

$$S'_{-2} = -S'_{+2} + \sqrt{\frac{2}{\tau_2'}}\,a_2. \quad (16)$$

Here, ω_i and τ_i, $i = 1, 2$ are the frequencies and the decaying time of the two cavities, respectively, S_{+i} and S_{-i} are the incoming and outgoing waves for the ith cavity at either the input or the output waveguide, while S'_{+i} and S'_{-i} are the incoming and outgoing waves for the ith cavity in the connecting waveguide. Furthermore, due to the wave propagation within the waveguide, we have

$$S'_{+2} = e^{j\varphi}S'_{-1} \quad (17)$$

and

$$S'_{+1} = e^{j\varphi}S'_{-2}. \quad (18)$$

Combining (14), (16)–(18), we have

$$S'_{+1} = j\frac{-a_1 e^{j\varphi}\sqrt{\frac{2}{\tau_1'}} + a_2\sqrt{\frac{2}{\tau_2'}}}{2\sin\varphi} \quad (19)$$

and

$$S'_{+2} = -j\frac{-a_1\sqrt{\frac{2}{\tau_1'}} + a_2 e^{j\varphi}\sqrt{\frac{2}{\tau_2'}}}{2\sin\varphi} \quad (20)$$

which can be plugged back into (11) and (12) to determine an effective coupling constant between the two cavities. In this way, one could write the coupling constant between the two cavities as

$$\kappa_{12} = \left[-\frac{a_1}{\tau_1'}\left(1 + \frac{je^{j\varphi}}{\sin\varphi}\right) + \frac{ja_2}{\sin\varphi\sqrt{\tau_1'\tau_2'}}\right]\Big/ a_2 \quad (21a)$$

$$\kappa_{21} = \left[-\frac{a_2}{\tau_2'}\left(1 + \frac{je^{j\varphi}}{\sin\varphi}\right) + \frac{ja_1}{\sin\varphi\sqrt{\tau_1'\tau_2'}}\right]\Big/ a_1 \quad (21b)$$

Comparing (21) with (10), we see that the criterion outlined above can indeed be achieved with $\varphi = 2n\pi + \pi/2$, $\tau_1 = \tau_1'$, and $\tau_2 = \tau_2'$. Therefore, it can be deduced that $\kappa_{ij}\kappa_{ji} = -|\kappa_{ij}|^2 = -|\kappa_{ji}|^2 = 1/\tau_i\tau_j$. Thus, ideal performance for our demultiplexer can be realized by using a symmetric waveguide and a symmetric branch, and by choosing the appropriate phase shift between the branch and the high-Q cavities.

We note that, in general, the phase φ is frequency dependent. However, since the entire signal bandwidth is typically only on the order of a few percent of the carrier frequency, the variation of φ over the entire signal bandwidth should be small. Also, in general the phase shift can only determined by detailed electromagnetic simulations. The analytic calculations above however establish the basic criteria for the design procedure. Finally, for our purposes here, the choice of phase factor at $\varphi = 2n\pi + \pi/2$ avoids the diverging point of the coupling constant κ and therefore leads to a simplified formalism. In the cases where $\varphi = n\pi$, the coupling constant between the cavities diverge, and it is no longer appropriate to describe the system in terms of the coupling coefficients κ. However, even in this case, there is still a valid physical solution to (11)–(16). Such a physical solution corresponds to the situation where the resonant amplitudes in the two resonators oscillates exactly in phase.

We shall emphasize that a symmetric branch, as characterized by equal decay of the resonance to each of the branches, generates a finite reflection [16] by itself. In this design, it is precisely this finite reflection from the branch that cancels the reflected amplitude from the high-Q resonances, resulting in an overall reflectionless operation at every frequency channel for the demultiplexer.

To visualize the behavior of our analytic theory, we plot the results of equations (5)–(7) in Fig. 4, in the regime where the criteria (8)–(10) are satisfied. For concreteness, we have arbitrarily chosen the normalized resonant frequencies and decay rates (ω_1, $1/\tau_1$), (ω_2, $1/\tau_2$), and (ω_3, $1/\tau_3$) as (1.0, 0.5), (1.04, 0.0005), and (0.96, 0.0005), respectively. It can be found that t_2 and t_3 indeed approach 100% at the resonant frequencies, while the reflection vanishes at these frequencies. Thus, our theory does indeed predict the presence of an ideal demultiplexer.

We can generalize the results, as described above for a two-channel demultiplexer, to a system with N output ports. The structure is shown in Fig. 5, where each port outputs a specific frequency channel. Using similar theoretical derivations,

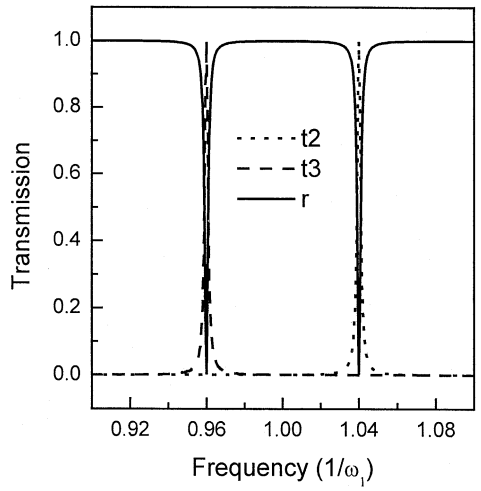

Fig. 4. Transmission spectra for a two-channel wave demultiplexer, as shown in Fig. 2(a). assuming that $(\omega_1, 1/\tau_1)$, $(\omega_2, 1/\tau_2)$ and $(\omega_3, 1/\tau_3)$ are (1.0, 0.5), (1.04, 0.0005), (0.96, 0.0005) respectively.

the transmittivity at a particular port P_i can be expressed as in (22), shown at the bottom of the page.

Equation (22) describes a system that is represented in Fig. 1(a). To apply (22) to a system as shown in Fig. 5, we note that the essence of the derivation is the presence of a symmetric branch with the reflection amplitude equal to the transmission amplitude into the each of the branch. It is, therefore, conceivable that such a branching structure can be built with a tree-like structure. We will investigate this further in later works.

From (22), it can be clearly seen that, at a frequency channel $\omega = \omega_i$, when the criteria as described by (8)–(10) are satisfied, the transmittivities of all ports are zero except for port P_i, where it reaches 100%. No reflection can be found at the input port P_1 for all frequency channels. In order to visualize the propagation properties described by (22), the transmission spectra of each port in a 16-channel wave demultiplexer are plotted in Fig. 6, where assuming that $1/\tau_1$ is 0.5, $1/\tau_i$ $(i = 2 \sim 17)$ is 0.0001. It is clear that the transmittivity at each port does approach 100% at resonant frequency. That is an N channels wave demultiplexer.

To test the validity of the above approach, the multiple scattering method [19], [20] is employed to simulate the propagation of waves in these structures. An experiment in the microwave region is also carried out, the detailed experiment setup can be found elsewhere [21]. Here, we adopt the structure as shown in Fig. 2(a), the parameters of this photonic crystal wave demultiplexer are chosen as follows. The photonic crystal with a lattice constant a is composed of $0.182a$ radius dielectric cylinders imbedded in a background dielectric medium. The dielectric constants of the cylinders and background are 8.0

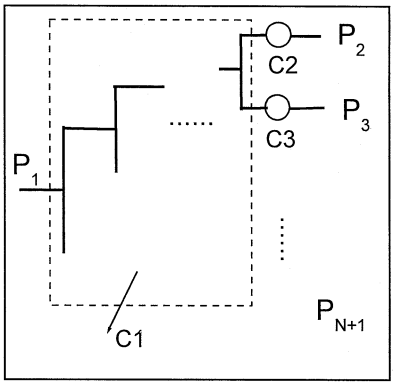

Fig. 5. Schematic optical circuit for realizing N channels wave demultiplexer in two-dimensional photonic crystal.

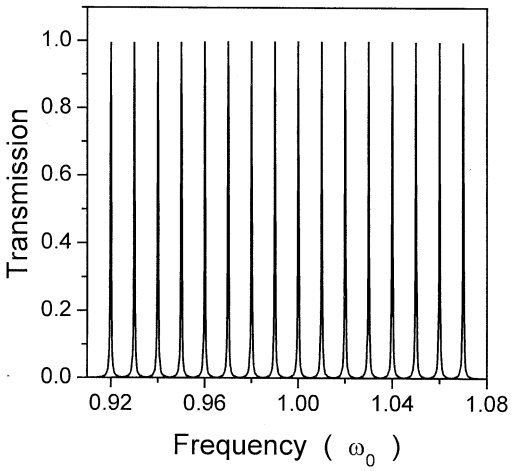

Fig. 6. Transmission spectra for a 16-channel wave demultiplexer assuming that $1/\tau_1$ is 0.5 and $1/\tau_i$ $(i = 2 \sim 17)$ is 0.0001.

and 1.03. respectively. The first band gap of this crystal for S-polarized waves is in the range of $0.36 \sim 0.46 c/a$, where c is the light velocity in vacuum. Point defect is created by replacing a selected cylinder with a dielectric cylinder with different radius and dielectric constant. C_2 and C_3 are two special cylinders and serve as two point defects, and their radius and dielectric constants are $0.182a$, 1.0 and $0.273a$, 8.0 respectively. In the simulation, we integrate the energy fluxes at two outlets respectively. Meanwhile, the energy flux at the outlet of a corresponding straight waveguide shown in Fig. 2(b) is also calculated. For clarity, we define a renormalized transmission spectrum, which is a ratio of the flux at the outlet of the demultiplexer to that of the straight waveguide from each outlet. From the spectrum. one can confirm whether the reflection from the input port exists at the peak frequencies. The measured and simulated transmission spectra are plotted

$$t_i = \left|\frac{S_{-i}}{S_{+i}}\right|^2 = \left|\frac{\frac{2\kappa_{i1}}{\sqrt{\tau_1\tau_i}}}{\left[j(\omega-\omega_1)+\frac{1}{\tau_1}\right]\left[j(\omega-\omega_i)+\frac{1}{\tau_i}\right]+|\kappa_{1i}|^2+\sum\limits_{m\neq 1,i}|\kappa_{1m}|^2\frac{\left[j(\omega-\omega_i)+\frac{1}{\tau_i}\right]}{\left[j(\omega-\omega_m)+\frac{1}{\tau_m}\right]}}\right|^2 \tag{22}$$

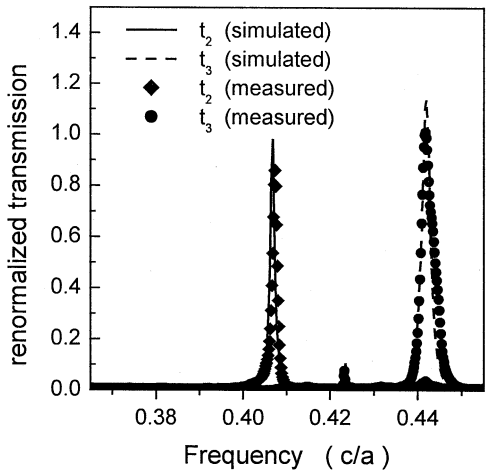

Fig. 7. Measured and simulated renormalized transmission spectra at the outlets of the demultiplexer.

in Fig. 7, where diamond and solid circles are the experimental values obtained from P_2 and P_3 ports, respectively, while the solid and dashed lines are the corresponding simulations. It is found that the transmission to the P_2 port exhibits a single Lorentzian peak at a resonant frequency of 0.4420 (c/a), while the transmission to P_3 port also shows a single Lorentzian peak at a resonant frequency of 0.4068 (c/a). Moreover, both peaks have their maximal transmissivity approaching 100%. Because both simulations and experiments presented in this paper incorporate the reflection from the interfaces at the edges of the crystal and therefore does possess some error that over 100% transmission appears at the peak of the port–3 spectrum. However, the presence of large transmitted amplitudes at both frequencies is a strong and clear evidence that the cancellation of reflection amplitude is at work here. From energy-conservation considerations, the existence of a near-complete transmission at these two frequencies indicates that the reflection is small for *both* frequencies for the structure. Furthermore, both the experimental and simulated results agree well with each other, except that there exists a little peak in both of P_2 and P_3 ports which might be caused by very small interaction between microcavities C_2 and C_3. These facts reveal that directly coupling resonant tunneling effect can be used to design wavelength demultiplexer with no reflection at the peak frequencies.

In conclusion, we introduce a wavelength demultiplexer operating by the coupling among a low-quality factor cavity and N microcavities with high-quality factors. This optical circuit is similar to the low-frequency multichannel filter electronic circuit. The merit of this optical circuit is that the design of such a circuit is very simple because one might build a defect to extract a peak frequency and the technological complexity is reduced compared with the channel drop tunneling wave demultiplexer. Furthermore, the reflection at the peak frequencies can be fully eliminated compared with the other method where considerable reflection appears. Even though our simulation and experiment are working in a two-dimensional photonic crystal, our theory based on the coupling theory can be valid for both two- and three-dimensional photonic crystals. This method might also be valuable for the design of other all-optical functional circuits.

ACKNOWLEDGMENT

The authors would like to thank Prof. Z. Zhang from HKUST for his program of multi-scattering method. They also thank the National Research Center for Intelligent Computing System for use of the Dawning-2000A parallel computer.

REFERENCES

[1] C. Dragone, "Efficient $n \times n$ star couplers using Fourier optics," *J. Lightwave Technol.*, vol. 7, pp. 479–489, 1989.
[2] H. A. Haus and Y. Lai, "Narrow-band optical channel-dropping filter," *J. Lightwave Technol.*, vol. 10, pp. 57–62, 1992.
[3] H. Takahashi, S. Suzuki, and I. Nishi, "Wavelength multiplexer based on SiO_2–Ta_2O_5 arrayed-waveguide grating," *J. Lightwave Technol.*, vol. 12, pp. 989–995, 1994.
[4] K. Hill, Y. Fujii, D. C. Johnson, and B. S. Kawasaki, "Photosensitivity in optical fiber waveguides: application to reflection filter fabrication," *Appl. Phys. Lett.*, vol. 32, pp. 647–649, 1979.
[5] S. Fan, P. R. Villeneuve, and J. D. Joannopoulos, "Channel drop tunneling through localized states," *Phys. Rev. Lett.*, vol. 80, pp. 960–963, 1998.
[6] S. Fan, P. R. Villeneuve, J. D. Joannopoulos, M. J. Khan, C. Manolatou, and H. A. Haus, "Theoretical analysis of channel drop tunneling process," *Phys. Rev. B*, vol. 59, pp. 15 882–15 892, 1999.
[7] C. Manolatou, M. J. Khan, S. Fan, P. R. Villeneuve, H. A. Haus, and J. D. Joannopoulos, "Coupling of modes analysis of resonant channel add–drop filters," *IEEE J. Quantum Electron.*, vol. 35, pp. 1322–1331, 1999.
[8] S. Noda, A. Chutinan, and M. Imada, "Trapping and emission of photons by a single defect in a photonic bandgap structure," *Nature*, vol. 407, pp. 608–610, 2000.
[9] A. Chutinan, M. Mochizuki, M. Imada, and S. Noda, "Surface-emitting channel drop filters using single defects in two-dimensional photonic crystal slabs," *Appl. Phys. Lett.*, vol. 79, pp. 2690–2692, 2001.
[10] A. Sharkawy, S. Shi, and D. W. Prather, "Multichannel wavelength division multiplexing with photonic crystals," *Appl. Opt.*, vol. 40, pp. 2247–2252, 2001.
[11] H. Kosaka, T. Kawashima, A. Tomita, M. Notomi, T. Tamamura, T. Sato, and S. Kasakami, "Photonic crystals for microlightwave circuits using wavelength-dependent angular beam steering," *Appl. Phys. Lett.*, vol. 74, pp. 1370–1372, 1999.
[12] E. Yablonovitch, "Inhabited spontaneous emission in solid-state physics and electronics," *Phy. Rev. Lett.*, vol. 58, pp. 2058–2062, 1987.
[13] S. John, "Strong localization of photons in certain disordered dielectric superlattices," *Phys. Rev. Lett.*, vol. 58, pp. 2486–2489, 1987.
[14] J. Joannopoulos, R. D. Meade, and J. Winn, *Photonic Crystals*. Princeton, NJ: Princeton Univ., 1995.
[15] J. Davidse, *Analog Electronic Circuit Design*. Englewood Cliffs, NJ: Prentice-Hall, 1991.
[16] S. Fan, S. G. Johnson, J. D. Joannopoulos, C. Manolatou, and H. A. Haus, "Waveguide branches in photonic crystals," *J. Opt. Soc. Amer. B*, vol. 18, pp. 162–166, 2001.
[17] H. A. Haus, *Waves and Fields in Optoelectronics*. Englewood Cliffs, NJ: Prentice-Hall, 1984.
[18] H. A. Haus and Y. Lai, "Theory of cascaded quarter wave shifted distributed feedback resonators," *IEEE J. Quantum Electron.*, vol. 28, pp. 205–213, 1992.
[19] L. M. Li and Z. Q. Zhang, "Multiple-scattering approach to finite-sized photonic band-gap materials," *Phys. Rev. B*, vol. 58, pp. 9587–9590, 1998.
[20] D. Felbaq, G. Tayeb, and D. Maystre, "Scattering by a random set of parallel cylinders," *J. Opt. Soc. Amer. A*, vol. 11, pp. 2526–2538, 1994.
[21] C. Jin, B. Cheng, B. Man, D. Zhang, S. Ban, B. Sun, L. Li, and Z. Zhang, "Two-dimensional metallodielectric photonic crystal with a large band gap," *Appl. Phys. Lett.*, vol. 75, pp. 1201–1203, 1999.

Chongjun Jin was born in Zhejiang Province, China, in 1969. He received the Ph.D. degree in physics from Harbin Institute of Technology, Harbin, China, in 1997.

He has been with the Institute of Physics, Chinese Academy of Sciences, Beijing, China, since 1997, where he is currently an Associate Research Scientist. He is also a Research Assistant at the Department of Electrical and Electronics Engineering, University of Glasgow, Glasgow, U.K. His main research interests are as follows: applications of photonic crystals in the fields of optoelectronics, preparation of three-dimensional photonic crystals through the self-assembly method, nonlinear effects of photonic crystals, simulation of the propagation of electromagnetic waves in photonic crystals, and preparation of two-dimensional photonic crystals using wet and dry etching.

Shanhui Fan received the Ph.D. degree in physics from the Massachusetts Institute of Technology (MIT), Cambridge, in 1997.

He has been an Assistant Professor of Electrical Engineering at Stanford University since 2001. Previously, he was a Research Scientist at the Research Laboratory of Electronics, MIT. His research interests are in computational and theoretical studies of the basic properties and applications of micro- and nano-photonic structures. He has published 47 journal articles, has given more than 20 invited talks at U.S. and international conferences, and holds 11 patents.

Dr. Fan is a member of the American Physical Society and the Optical Society of America.

Shouzhen Han was born in Hebei Province, China, in 1976. He received the Master's degree from Beijing Polytechnic University, Beijing, China, in 2002. He is currently working toward the Ph.D. degree at the Institute of Physics, Chinese Academy of Sciences, Beijing, China.

Daozhong Zhang was born in Sichuan Province, China, in 1943. He graduated from the Chinese University of Science and Technology in 1965.

Since then, he has been with the Institute of Physics, Chinese Academy of Sciences, Beijing, China, where he is currently a Research Scientist and the Director of the Optical Physics Laboratory. His research interests include laser spectroscopy of atoms and molecules, nonlinear optics, photonic crystals, and light localization. He has published more than 100 papers.